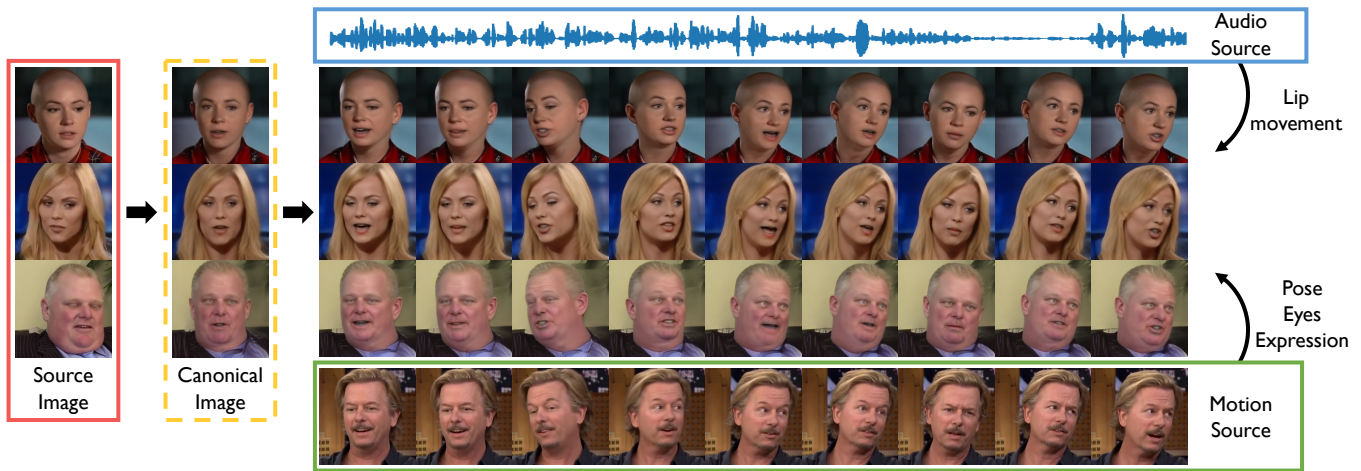


# THAT'S WHAT I SAID: FULLY-CONTROLLABLE TALKING FACE GENERATION

Youngjoon Jang<sup>1\*</sup>, Kyeongha Rho<sup>1\*</sup>, Jong-Bin Woo<sup>1</sup>, Hyeongkeun Lee<sup>1</sup>,  
Jihwan Park<sup>2,3</sup>, Youshin Lim<sup>2,3</sup>, Byeong-Yeol Kim<sup>2,3</sup>, Joon Son Chung<sup>1</sup>

<sup>1</sup>Korea Advanced Institute of Science and Technology, Daejeon, Republic of Korea  
<sup>2</sup>Hyundai Motor Company, <sup>3</sup>42dot Inc., Seoul, Republic of Korea

Project page with demo: <https://mm.kaist.ac.kr/projects/FC-TFG>



**Figure 1:** Our novel talking face generation framework precisely reflects every facial expression of the motion source while synchronising the lip shape with the input audio source. The key to our framework is to find the canonical space, where every face has the same motion patterns but different identities.

## ABSTRACT

The goal of this paper is to synthesise talking faces with controllable facial motions. To achieve this goal, we propose two key ideas. The first is to establish a canonical space where every face has the same motion patterns but different identities. The second is to navigate a multimodal motion space that only represents motion-related features while eliminating identity information. To disentangle identity and motion, we introduce an orthogonality constraint between the two different latent spaces. From this, our method can generate natural-looking talking faces with fully controllable facial attributes and accurate lip synchronisation. Extensive experiments demonstrate that our method achieves state-of-the-art results in terms of both visual quality and lip-sync score. To the best of our knowledge, we are the first to develop a talking face generation framework that can accurately manifest full target facial motions including lip, head pose, and eye movements in the generated video without any additional supervision beyond RGB video with audio.

\*These authors contributed equally to this work.

## 1. INTRODUCTION

Audio-driven talking face generation technology has numerous applications in the film and entertainment industry, including virtual assistants, video conferencing, and dubbing. Its aim is to generate animated faces that closely match the audio, creating more engaging experiences for users. This technology has the potential to revolutionize industries by making human-machine interactions more natural and immersive.

Previous literature on deep learning-based talking face synthesis can be divided into two branches. The first branch [1, 2, 3, 4, 5, 6, 7, 8] only uses RGB modality as a form of supervision to reconstruct a target video, while the second branch [9, 10, 11, 12, 13, 14, 15, 16, 17, 18, 19] leverages 2D or 3D structural information to propagate more specific and detailed supervision. These works have made significant progress in generating natural-looking lip motions. Nevertheless, there is still a need for further development in controlling head pose and refining facial attributes in greater detail.

Recent methods [20, 21, 22] have the ability to generate

talking faces that closely resemble the movements and identities from a target video. However, these methods still have limitations. For instance, [20] is only capable of altering the head pose, while [22] is incapable of creating detailed facial components like eye gaze movements. [21] requires the utilisation of facial keypoints to physically separate facial components such as eyes, lips, and other facial areas to create varied expressions with a clean background. This approach is limited in its deployment to real-world applications.

In this paper, we propose a novel framework, Fully-Controllable Talking Face Generation (FC-TFG), which aims to address the limitations of existing methods by generating talking faces with full target motion, including head pose, eyebrows, eye blinks, and eye gaze movements, without the need for additional supervisions such as facial keypoints.

We leverage a pre-trained face image generator and an inversion network. By utilising the pre-trained generator, we can generate exceptionally high-quality facial images that retain natural appearance and expression, while the inversion network helps map these images back to the latent space for manipulation of specific facial features and expressions. This approach ensures that the talking faces produced by our model are not only semantically coherent and authentic but also incredibly realistic and visually stunning.

To achieve effective navigation and manipulation of the pre-trained generator’s latent space, we aim to disentangle the latent space into two distinct subspaces: a canonical space that can accommodate a variety of facial identities while maintaining consistent facial attributes, and a multimodal motion space that contains exclusively motion features acquired by fusing both audio and image sources for transferring the target’s motion to the source face image.

To establish a more distinct disentanglement between the two latent spaces, we introduce a constraint that enforces orthogonality between the canonical space and the multimodal motion space. This constraint ensures that the canonical features, which capture person-specific characteristics such as facial shape and texture, are completely independent of the multimodal motion features, which encode the target motion such as head pose, facial expression, and eye gaze.

By enforcing orthogonality between the canonical space and the multimodal motion space, our method can generate more controllable facial animations, while avoiding unwanted mixing of different types of conditions. Additionally, discovering the canonical space changes the motion relationships between source and target images from relative motion to absolute motion, which is easier for the model to learn. As a result, we can resolve the complex motion connections with a straightforward linear operation. The proposed method can be particularly useful for applications that require fine-grained control over different facial features, such as virtual communication, social robotics, and entertainment.

In summary, we make three key contributions: (1) We propose a novel framework, Fully-Controllable Talking Face

Generation (FC-TFG), that generates talking faces with controllable target motion, including head pose, eyebrows, eye blinks, eye gaze, and lip movements. (2) We separate the style latent space into a canonical space that contains only person-specific characteristics and a multimodal motion space that contains person-agnostic motion features encoded from driving pose video and audio source. By imposing an orthogonality constraint on the correlation between the two spaces, the proposed model produces detailed and controllable facial animation. (3) We demonstrate that the proposed FC-TFG is highly effective in generating talking faces with sophisticated motion control, producing state-of-the-art results in both qualitative and quantitative metrics. This success highlights the potential of FC-TFG for a wide range of applications that demand precise control over various facial features.

## 2. RELATED WORKS

### 2.1. Audio-Driven Talking Face Generation.

The synthesis of speech-synchronised video portraits has been a significant area of research in computer vision and graphics for many years [23, 24]. Early works [25, 26] focus on the individual speaker setting where a single model can generate various talking faces corresponding to only one identity. Recently, the development of deep learning enables the design of more generalised talking face generation models [1, 6, 27, 4, 16, 7, 8] that produce talking faces by inputting identity conditions. However, these works neglect head movements since disentangling head poses from identity-related facial characteristics is challenging.

To produce talking face videos that have dynamic and natural movements, some studies utilise landmarks or mesh information [11, 10, 14, 13, 28].

For the similar purpose, some works [29, 30, 31, 32, 19] adopt 3D information as intermediate representations. Even with additional modalities, the proposed models have certain limitations such as lacking pose control and the inability to render faces with visually pleasing quality under one-shot conditions. Additionally, they suffer from severe performance degradation in situations where the accuracy of landmarks is low, especially in the wild.

Several recent works [20, 21, 22, 33] have demonstrated that it is possible to create realistic talking faces that mimic different movements and identities from a target video. However, there are a number of limitations: [20] can only modify head pose, [21] requires segmentation masks to erase backgrounds, [22] cannot animate eye gazes, and [21] requires facial keypoints to disentangle visual information for generating varied expressions in a background-removed setting.

Unlike the previous works, our framework can generate a wide range of target expressions including pose, lip, eye blink, and even eye gaze without requiring extra annotations or structural information. Our framework seeks a canonical

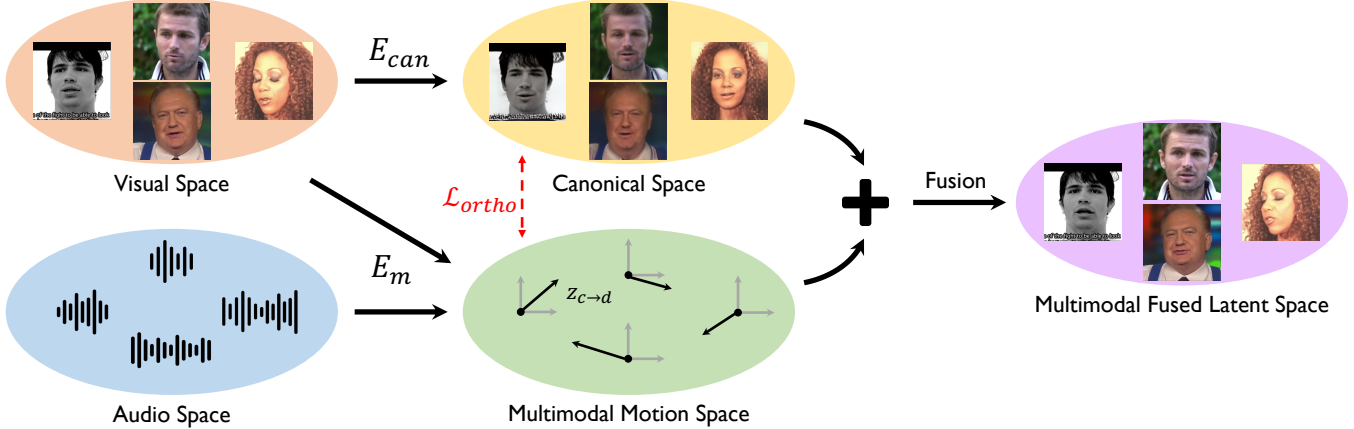


**Figure 2: Overall framework.** Our goal is to transfer the motions of the individual portrait via latent space exploration. The overall pipeline is comprised of two steps. The first step involves transferring the code in the style latent space to the canonical latent space, where each face has the same facial attributes, but with distinct identities. In the second step, the multimodal motion space is navigated, where each code contains only motion information and excludes identity information. The target motion code is obtained by fusing image latent features and audio latent features. The canonical code and the motion code are then combined using a linear operation, resulting in the final multimodal fused latent code. This fused latent code is used as input to the decoder to synthesise attribute-controllable talking face videos.

space of a generator, where each face has the same lip shape and pose, but different identities. This method enables the creation of more advanced facial representations and simplifies the modeling of motion transfer between source and target images by changing their motion relationship from relative to absolute. Additionally, our model consistently produces high-quality videos under one-shot conditions.

## 2.2. Latent Space Editing.

Latent space editing involves intentionally modifying the generated output results by exploring meaningful directions in the latent space of a pre-trained generator network. These directions enable linear navigation that corresponds to desired image manipulation. To manipulate the latent space, some approaches [34, 35, 36] directly propagate labeled supervision such as facial attributes. Other studies [37, 38, 39, 40] modify the semantics of images without labeled data.

In contrast to finding directions that correspond to individual face attributes by using a single modality, our work aims to disentangle the face identity and the complex attributes composing face motions with multimodal features representing visual and audio information.

## 3. METHOD

In this work, we propose a self-supervised approach for generating talking face videos that can transfer complex motions such as head poses and eye blinks from a driving video to a source identity image. Such motion transformation is modeled via disentangled latent feature manipulation. The pro-

posed framework’s pipeline is illustrated in Fig. 2. The key to our framework is two mapping operations: (1) Visual Space to Canonical Space, (2) Visual/Audio Space to Multimodal Motion Space. Through the first mapping, we obtain canonical images that have the same motion features and different identities. Meanwhile, the second mapping yields motion vectors that enable us to transfer desired motions onto canonical images. To ensure the disentanglement of the two subspaces, we impose an orthogonality constraint. Based on this process, our model is capable of generating talking faces that mimic the facial motion of the target.

We further provide an overview of the proposed framework in Fig. 3. Our framework includes a visual encoder  $E_{inv}$ , an audio encoder  $E_a$ , a generator  $G$ , a discriminator  $D$ , and a Latent Fusion Network. We adopt a single shared visual encoder to extract both source and driving latent codes, denoted as  $z_s$  and  $z_d$ , respectively. The audio encoder extracts an audio latent code,  $z_a$ . The canonical encoder  $E_{can}$  maps  $z_s$  to a canonical code, denoted as  $z_{s→c}$ , which is then combined with a motion code  $z_{c→d}$  obtained from the multimodal motion encoder  $E_m$ . Since an orthogonality constraint is imposed between  $z_{s→c}$  and  $z_{c→d}$ , the motion transfer process is implemented by simply adding the two latent codes. To ensure generated motions are natural, the fused code  $z_{s→d}$  is passed through a Temporal Fusion layer before being fed into the generator  $G$ . The generator, which is the StyleGAN2 decoder, allows for controlling the coarse-fine motion transfers.

Overall, the proposed method presents a promising approach for generating high-quality talking face videos with complex motions and controllability.

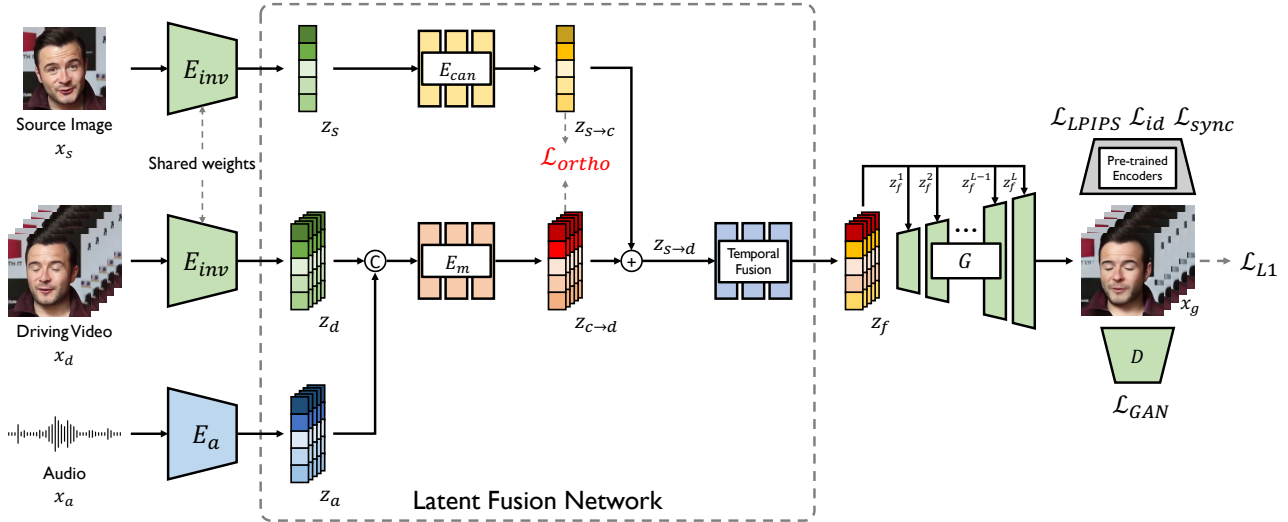


**Figure 3: Overall Architecture of FC-TFG.** Our model consists of several components, including a visual encoder  $E_{inv}$ , an audio encoder  $E_a$ , a generator  $G$ , a discriminator  $D$ , and Latent Fusion Network. For compactness, we use a single visual encoder to extract both a source latent code  $z_s$  and a driving latent code  $z_d$ . The audio encoder extracts an audio latent code  $z_a$ . First, we design a canonical encoder  $E_{can}$  to map  $z_s$  to a canonical space as  $z_s \rightarrow z_{s \rightarrow c}$ , and then linearly combine it with a target motion code  $z_{c \rightarrow d}$ . This motion code is produced by a multimodal motion encoder  $E_m$ , which combines  $z_d$  and  $z_a$ . To generate natural motions, we pass the target code through a Temporal Fusion layer before feeding it into the generator  $G$ . The generated video  $x_g$  is compared to a driving video  $x_d$  based on its visual and synchronisation quality. Note that we employ the StyleGAN2 generator as a decoder to control coarse-fine motion transfers, and  $L$  is the number of modulation layers of the generator. Therefore, each model ( $E_{can}$  and  $E_m$ ) in Latent Fusion Network has  $L$  independent weights.

### 3.1. Navigating Canonical Space

Our main target is to obtain a latent code  $z_{s \rightarrow d; t} \sim \mathcal{Z} \in \mathbb{R}^N$  that captures the motion transformation from the source image  $x_s$  to the  $t$ -th driving frame  $x_{d; t}$ . From now on, we omit temporal index  $t$  for readability. Directly seeking  $z_{s \rightarrow d}$  in the latent space is challenging because the model should be able to capture a relative motion relationship between  $x_s$  and  $x_d$  while representing detailed facial attributes. To address this issue, we adopt an alternative approach by assuming the presence of a canonical image  $x_c$  in a canonical space which is a latent space having unified face-related motions but individual identities. Then, we can acquire the target mapping code  $z_{s \rightarrow d}$  through the following 2-stage motion transfer.

$$z_{s \rightarrow d} = z_{s \rightarrow c} + z_{c \rightarrow d}, \quad (1)$$

where  $z_{s \rightarrow c}$  and  $z_{c \rightarrow d}$  indicate the transformation  $x_s \rightarrow x_c$  and  $x_c \rightarrow x_d$  respectively. Now, the mapping  $z_{s \rightarrow d}$  is solved using absolute motion transfer, where both  $z_{s \rightarrow c}$  and  $z_{c \rightarrow d}$  do not need to account for the motion relationship between them. To design this motion transfer process effectively and intuitively, we apply a simple linear operation that adds  $z_{c \rightarrow d}$  directly to  $z_{s \rightarrow c}$ . Here,  $z_{s \rightarrow c}$  is obtained by passing  $z_s = E_{inv}(x_s)$  through  $E_{can}$  which is a 2-layer MLP, and  $z_{c \rightarrow d}$  is learned by navigating motion space that will be further explained in the following section.

### 3.2. Navigating Multimodal Motion Space

To generate natural head poses, lip motions, and facial expressions simultaneously,  $z_{c \rightarrow d}$  should successfully combine both vision and audio information while only containing motion-related features. To disentangle identity-related codes and motion-related codes in  $N$ -dimensional latent space, We inject channel-wise orthogonality constraint into each channel in  $z_{s \rightarrow c}$  and  $z_{c \rightarrow d}$ . By enforcing this constraint, the model induces that the identity and motion codes do not interfere with each other when they are combined for the transformation with the linear operation as explained in Sec. 3.1.  $z_{c \rightarrow d}$  can be obtained as follows:

$$z_{c \rightarrow d} = E_m(E_a(x_a) \oplus E_{inv}(x_d)), \quad (2)$$

where  $E_a$ ,  $E_m$ , and  $x_a$  denote audio encoder, motion encoder, and audio input respectively.  $\oplus$  operation indicates channel-wise concatenation. Note that as we solely traverse the latent space of the pre-trained image decoder, the resulting  $z_{s \rightarrow d}$  can retain semantically meaningful features. The structure of the motion encoder is a 3-layer MLP. Finally, to generate temporally consistent latent features, we refine the acquired  $z_{s \rightarrow d}$  by feeding it to the Temporal Fusion layer, which consists of a single 1D convolutional layer.

### 3.3. Training Objectives

#### 3.3.1. Orthogonality loss.

To guarantee that disentangling  $z_{s \rightarrow c}$  and  $z_{c \rightarrow d}$  to control the generated talking faces, we make slight modifications to the orthogonality loss introduced in [40]. We add a division term  $N$  which is the number of channels of the latent code to ensure a consistent loss scale during training. The modified loss is expressed as follows:

$$\mathcal{L}_{ortho} = \frac{1}{N} \sum (z_{s \rightarrow c} \odot z_{c \rightarrow d}), \quad (3)$$

where  $\odot$  indicates Hadamard product operation.

#### 3.3.2. Synchronisation loss.

To generate well-synchronised videos  $x_g$  with the input audio conditions, we adopt a sync loss function, which utilises a pre-trained SyncNet [42] comprising an audio encoder and a video encoder. Many previous works [22, 8, 7, 19, 32] utilise modified versions of SyncNet with altered objective functions, to improve lip-sync quality. We use a modified SyncNet introduced in [22] to enhance the lip representations.

The distance between the features of a video and its synchronised audio, extracted from the pre-trained Syncnet model, should be close to 0. From this, we minimise the following sync loss:

$$\mathcal{L}_{sync} = 1 - \cos(f_v(x_g), f_a(x_a)), \quad (4)$$

where  $f_a$  and  $f_v$  denote the audio encoder and video encoder of SyncNet respectively.

#### 3.3.3. Identity loss.

To preserve facial identity after motion transformation, we apply an identity-based similarity loss [43] by employing a pre-trained face recognition network  $E_{id}$  [44].

$$\mathcal{L}_{id} = 1 - \cos(E_{id}(x_g), E_{id}(x_d)). \quad (5)$$

#### 3.3.4. Reconstruction loss.

For the reconstruction loss, we adopt L1 loss function that calculates the pixel-wise L1 distance between the generated talking face image,  $x_g$ , and the target image,  $x_d$ . The reconstruction loss can be calculated as follows:

$$\mathcal{L}_{rec} = \|x_g - x_d\|_1. \quad (6)$$

#### 3.3.5. Perceptual loss.

Using L1 reconstruction loss alone may result in blurry images or slight artifacts as it is a pixel-level loss. To compensate for the smoothing effect caused by the reconstruction loss

$\mathcal{L}_{L1}$ , we add the Learned Perceptual Image Patch Similarity (LPIPS) loss [45] as follows:

$$\mathcal{L}_{LPIPS} = \frac{1}{N_f} \sum_{i=1}^{N_f} \|\phi(x_g)_i - \phi(x_d)_i\|_2, \quad (7)$$

where  $\phi$  is a pre-trained VGG19 [46] network, and  $N_f$  is the number of feature maps.

#### 3.3.6. Adversarial loss.

We perform adversarial training with an image discriminator,  $D$ , to improve the quality of the generated videos. The architecture of  $D$  is the same as StyleGAN2 [47] discriminator. We use a non-saturating loss [48] for adversarial training, which can be expressed as follows:

$$\mathcal{L}_{GAN} = \min_G \max_D \left( \mathbb{E}_{x_d} [\log(D(x_d))] + \mathbb{E}_{z_f} [\log(1 - D(G(z_f)))] \right). \quad (8)$$

#### 3.3.7. Overall loss.

Our total loss can be formulated as follows:

$$\mathcal{L}_{total} = \lambda_1 \mathcal{L}_{ortho} + \lambda_2 \mathcal{L}_{sync} + \lambda_3 \mathcal{L}_{id} + \lambda_4 \mathcal{L}_{rec} + \lambda_5 \mathcal{L}_{LPIPS} + \lambda_6 \mathcal{L}_{GAN}, \quad (9)$$

where hyperparameters  $\lambda$  are introduced to balance the scale of each loss. Each  $\lambda$  controls the relative importance of its corresponding loss term. Empirically,  $\lambda_1, \lambda_2, \lambda_3, \lambda_4, \lambda_5$ , and  $\lambda_6$  are set to 1, 0.1, 0.5, 1, 1 and 0.1 respectively.

## 4. EXPERIMENTS

### 4.1. Experimental Setup

#### 4.1.1. Dataset.

Our framework is trained on VoxCeleb2 [49] and evaluated on both VoxCeleb2 and MEAD [50].

VoxCeleb2 includes 6,112 different identities and over 1 million utterances. Of the total identities, 5,994 are used for training, while the remaining identities are reserved for testing. We follow the pre-processing procedure proposed in [51] to ensure the consistent visual quality of videos.

To evaluate one-shot talking face generation performance, we utilise the MEAD dataset, which comprises emotional faces featuring more than 30 actors and eight emotion categories at three intensity levels. To conduct the evaluation, we randomly choose five speakers and five videos for each emotion category, and we only use the frontal-view videos from this dataset for testing purposes.

| Method          | Controllable Motions |      |           |          | VoxCeleb2       |                    |                 |                  |                  | MEAD            |                    |                 |                  |                  |
|-----------------|----------------------|------|-----------|----------|-----------------|--------------------|-----------------|------------------|------------------|-----------------|--------------------|-----------------|------------------|------------------|
|                 | lip                  | pose | eye blink | eye gaze | SSIM $\uparrow$ | MS-SSIM $\uparrow$ | PSNR $\uparrow$ | LMD $\downarrow$ | LSE-C $\uparrow$ | SSIM $\uparrow$ | MS-SSIM $\uparrow$ | PSNR $\uparrow$ | LMD $\downarrow$ | LSE-C $\uparrow$ |
| Wav2Lip [7]     | ✓                    | ✗    | ✗         | ✗        | 0.58            | -                  | 20.63           | 2.65             | <b>8.66</b>      | <b>0.85</b>     | -                  | 26.15           | 3.11             | <b>7.25</b>      |
| MakeItTalk [16] | ✓                    | ✗    | ✗         | ✗        | 0.55            | 0.45               | 16.94           | 3.28             | 3.83             | 0.78            | 0.78               | 23.6            | 3.55             | 4.35             |
| Audio2Head [41] | ✓                    | ✗    | ✗         | ✗        | 0.51            | 0.40               | 15.98           | 3.58             | 5.79             | 0.67            | 0.59               | 19.57           | 4.85             | 5.38             |
| PC-AVS [20]     | ✓                    | ✓    | ✗         | ✗        | 0.57            | 0.60               | 17.37           | 2.25             | 5.82             | 0.66            | 0.7                | 19.95           | 2.93             | 5.19             |
| FC-TFG (Ours)   | ✓                    | ✓    | ✓         | ✓        | <b>0.69</b>     | <b>0.77</b>        | <b>21.22</b>    | <b>1.58</b>      | 8.46             | 0.84            | <b>0.89</b>        | <b>26.19</b>    | <b>2.46</b>      | 5.51             |

**Table 1: Quantitative Results.** We compare our method to four publicly available baselines on six different metrics. Our approach outperforms the baseline methods in terms of both visual quality and lip synchronisation, while simultaneously controlling diverse and detailed facial motions. We evaluate the generated samples using the original authors’ experimental settings, ensuring a fair comparison between the different methods.

#### 4.1.2. Implementation Details.

We first train StyleGAN2 [47] generator on the VoxCeleb2 dataset and then train HyperStyle [52] inversion network with the pre-trained StyleGAN2 model. Specifically, we replace the e4e [53] encoder in the HyperStyle model with pSp [43] encoder. We focus on manipulating 8 specific layers of 14 layers in our generator, namely layers 1, 2, 3, 4, 7, 8, 9, and 10. Additionally, we only input the audio feature into 2 specific layers, layers 7 and 8. This allows us to effectively control the style of the generated images based on the audio input.

For the audio source, we downsample the audio to 16kHz, then convert the downsampled audio to mel-spectrograms with an FFT window size of 800, a hop length of 200, and 80 Mel filter banks. We utilise a pre-trained audio encoder introduced in [7] as our audio encoder. We use the Adam [54] optimiser for updating our model, with a learning rate of  $1e-4$ . Our framework is implemented on PyTorch [55] with eight 48GB A6000 GPUs. Note that the pre-trained models are fine-tuned during training.

#### 4.1.3. Comparison Methods.

We compare our method with several state-of-the-art talking face generation methods, which baselines are currently available. **Wav2Lip** [7] employs pre-trained SyncNet as a lip-sync discriminator to generate well-synchronised mouth region of the source image. **MakeItTalk** [16] predicts landmarks through 3D face models and generates both lip movements and head motions simultaneously driven by audio. **Audio2Head** [41] generates head motions by utilising a keypoint-based dense motion field driven by audio. **PC-AVS** [20] is a pose-controllable talking face generation model that generates head poses based on driving videos.

## 4.2. Quantitative Results

### 4.2.1. Evaluation Metrics.

We conduct quantitative evaluations with various metrics that have previously been adopted in the talking face generation field. To account for the accuracy of mouth shapes and lip

sync, we use Landmarks Distance (LMD) around the mouths proposed in [11], and Lip Sync Error Confidence (LSE-C) proposed in [42]. To compare the visual quality of the generated video, we use Structural Similarity Index Measure (SSIM) [56], Multi Scale Structural Similarity Index Measure (MS-SSIM) [57], and Peak Signal-to-Noise Ratio (PSNR).

### 4.2.2. Controllable Motion Types.

In order to assess the capabilities of the baseline methods in generating realistic talking faces, we compare the number of controllable motions for each method under the target conditions in Table Table 1. Wav2Lip, MakeItTalk, and Audio2Head rely solely on audio input to generate videos, resulting in limited control over motion and pose. In particular, MakeItTalk, and Audio2Head are capable of generating lip movements and small head pose variations that are synchronised with the audio conditions but are unable to produce more complex and diverse motion patterns. On the other hand, PC-AVS and Ours have the capacity to control head pose following the target pose conditions. However, while PC-AVS is limited to controlling head pose, our approach is effective for controlling all facial attributes, including eye blinks and gazes, by exploring disentangled latent spaces.

### 4.2.3. Evaluation Results.

We follow the evaluation protocol introduced in [20]. Specifically, we select the first frame of each test video to serve as a reference identity. We utilise the remaining frames to determine the subject’s pose, facial expression, and lip shape.

As shown in Table 1, we compare our method with four baselines on VoxCeleb2 and MEAD datasets. For VoxCeleb2 dataset, except for LSE-C metric, our proposed method surpasses the previous audio-driven and pose-controllable methods in all metrics while manipulating detailed facial components. For MEAD dataset, our framework shows the best performance on MS-SSIM, PSNR, and LMD and comparable results to the Wav2Lip model in terms of SSIM. Although the Wav2Lip model shows better performance on LSE-C metric, the generated face shows significant distortions. These

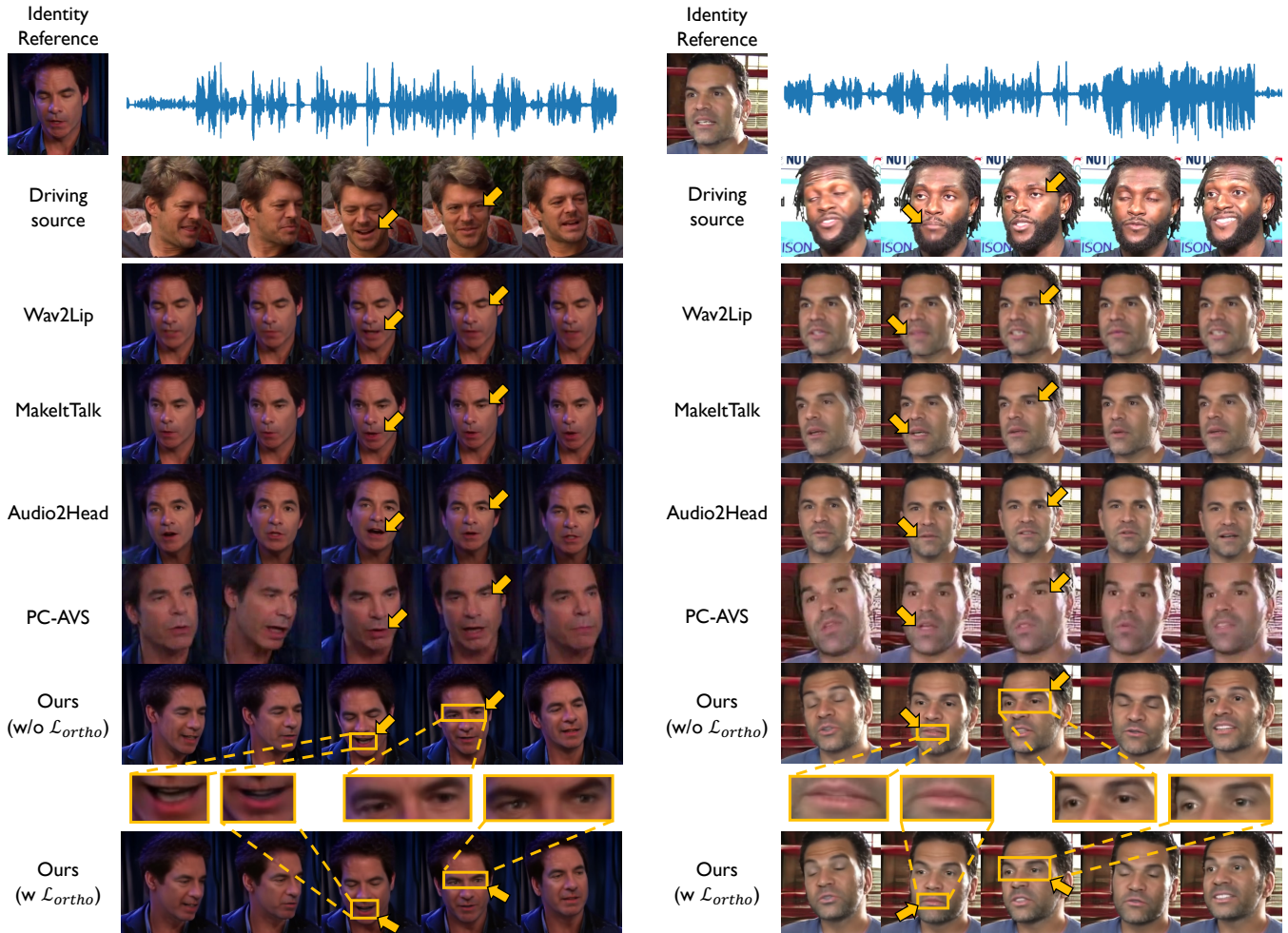


**Figure 4: Qualitative Results.** We compare our method with several baselines listed in Table 1. Our approach outperforms all the baselines in terms of generating precise head motion and facial expressions following the given conditions. Wave2Lip, MakeItTalk, and Audio2Head fail to generate accurate head motion of the driving source videos. PC-AVS produces a similar head pose with target motion but lacks in generating realistic facial expressions. On the other hand, our method successfully generates every facial expression of the target motion while synchronising the lip with the input audio source.

results demonstrate that our model is capable to capture detailed facial movements and generate visually pleasing results by keeping semantically meaningful the latent space.

### 4.3. Qualitative Results

#### 4.3.1. Fully-Controllable Talking Face Generation.

We visually show our qualitative results in Fig. 4. We clarify that Wav2Lip is a model that targets to change only lip region. MakeItTalk and Audio2Head are models that generate natural face motions conditioned by only audio source. For that reason, the generated videos can not follow diverse facial motions in the driving videos. PC-AVS focuses on synthesising the talking faces with controllable head pose variations. However, it fails to mimic the diving source’s facial expres-

sions such as eye blinks, eyebrows movements, and eye gazes. On the other hand, our method can generate fully-controllable talking faces by synthesising both head pose and facial expressions that precisely follow the driving source videos. In the example on the left of Fig. 4, following the yellow arrows, our model successfully captures the precise moment when the driving source smiles and reflects this expression on the generated face. Furthermore, as shown by the yellow arrows in the example on the right of Fig. 4, our model is able to replicate the eyebrows, forehead frowns, and eye gazes of the driving source. This level of detail and accuracy in replicating facial movements enables our method to generate highly realistic and expressive talking faces that closely follow the driving source’s emotions and expressions.

| Method                               | Wav2Lip | MakeItTalk | Audio2Head | PC-AVS | FC-TFG(Ours) |
|--------------------------------------|---------|------------|------------|--------|--------------|
| Lip Sync Quality $\uparrow$          | 3.47    | 2.31       | 2.55       | 3.29   | <b>3.93</b>  |
| Head Movement Naturalness $\uparrow$ | 1.88    | 2.5        | 2.98       | 3.23   | <b>4.14</b>  |
| Overall Quality $\uparrow$           | 2.18    | 2.64       | 2.91       | 2.91   | <b>3.94</b>  |

**Table 2: User Study.** We conduct a user study on generated videos with three aspects: lip synchronisation, the naturalness of head movement, and overall video quality. The higher the better, with the value range of 1 to 5.

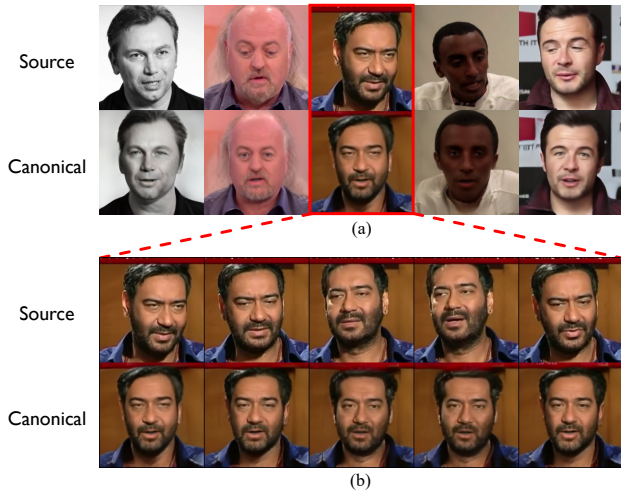


**Figure 5: Samples in Canonical Space.** We demonstrate how well our model preserves identity by mapping various identities to the canonical space. In Fig. (a), we generate diverse canonical image samples having different identities by feeding each canonical code to our generator. In Fig. (b), we further visualise every canonical image from a single video. These results prove that our model is robust to maintain the source identities and well-generalised to various identities.

#### 4.3.2. User Study.

We assess the quality of the videos generated by FC-TFG with a user study of 20 participants for their opinions on 20 videos. Specifically, we randomly collect reference images, driving videos, and driving audios from VoxCeleb2 [49] test split. Subsequently, we create videos based on Wav2Lip [7], MakeItTalk [16], Audio2Head [41], PC-AVS [20], and FC-TFG (Ours). We adopt the widely used Mean Opinion Scores (MOS) as an evaluation metric. The evaluation protocol closely follows [21, 20]. Each user gives evaluation scores from 1 to 5 for the following aspects of the generated videos: (1) lip sync quality; (2) head movement naturalness; and (3) video realism. Note that for a fair comparison with fully audio-driven generation methods, we do not include the metric that evaluates how well the poses of the generated faces match the poses of the driving videos. As shown in Table 2, it is demonstrated that our method generates talking face videos with higher lip synchronisation and natural head movement, compared to the existing methods.

| Temporal Fusion |              | $D$          |              | Metrics         |                    |                 |                  |                  |
|-----------------|--------------|--------------|--------------|-----------------|--------------------|-----------------|------------------|------------------|
| ID-Conv         | LSTM         | image        | video        | SSIM $\uparrow$ | MS-SSIM $\uparrow$ | PSNR $\uparrow$ | LMD $\downarrow$ | LSE-C $\uparrow$ |
|                 | $\checkmark$ | $\checkmark$ |              | 0.66            | 0.75               | 20.78           | 1.79             | <b>8.66</b>      |
|                 | $\checkmark$ |              | $\checkmark$ | 0.67            | 0.75               | 20.64           | 1.73             | 7.9              |
| $\checkmark$    |              |              | $\checkmark$ | 0.66            | 0.75               | 20.72           | 1.98             | 8.04             |
| $\checkmark$    |              | $\checkmark$ |              | <b>0.69</b>     | <b>0.77</b>        | <b>21.22</b>    | <b>1.58</b>      | 8.46             |

**Table 3: Ablations on Model Design.** We report performance results based on our different model choices. We observe that the highest performance is achieved when using a 1D convolutional layer for the Temporal Fusion layer and an image discriminator for the discriminator.

| Orthogonal Constraint | Metrics         |                    |                 |                  |                  |
|-----------------------|-----------------|--------------------|-----------------|------------------|------------------|
|                       | SSIM $\uparrow$ | MS-SSIM $\uparrow$ | PSNR $\uparrow$ | LMD $\downarrow$ | LSE-C $\uparrow$ |
| $\times$              | 0.67            | 0.76               | 20.88           | 1.70             | 8.27             |
| Cosine                | 0.67            | 0.75               | 21              | 2.11             | 8.38             |
| $L_{ortho}$           | <b>0.69</b>     | <b>0.77</b>        | <b>21.22</b>    | <b>1.58</b>      | <b>8.46</b>      |

**Table 4: Ablations on Orthogonality Loss.** We ablate the effectiveness of the orthogonality constraint.  $\times$  denotes the model trained without any orthogonality constraint.

## 4.4. Ablation Study

### 4.4.1. Canonical Space.

In Fig. 5 (a), we present the outcomes of mapping various identities to the canonical space *where each face has the same facial motion but different identities*. The effectiveness of our approach in preserving identity can be observed through the distinct and recognisable facial features of each individual. Additionally, as shown in Fig. 5 (b), regardless of the differences in the input images having the same identity, our approach consistently produces similar canonical images that accurately capture the individual’s distinct facial identity. These results further highlight the effectiveness of our method in finding the canonical space that is essential for transferring complex facial motions with a simple linear operation.

### 4.4.2. Ablations on Model Design.

We conduct ablation studies on our model choices for the Temporal Fusion layer and Discriminator  $D$ , as presented in Table 3. We empirically observe that a flickering phe-



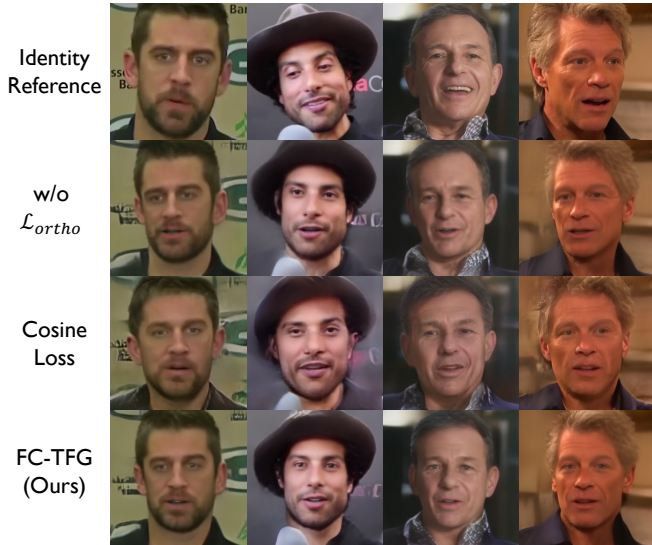


**Figure 6: Analysis on the effectiveness of Orthogonality Constraint.** Our model effectively disentangles the identity and motion information by enforcing orthogonality between the canonical space and the multimodal motion space. This is demonstrated by the cohesive and consistent motion patterns in the canonical space, which is not achieved in the models either trained without the orthogonality constraint or trained with other kinds of constraint such as cosine loss.

nomenon appears when using Long Short-Term Memory (LSTM) network as our temporal fusion model. We suspect that this issue is caused by our window size, which does not have any overlap along the temporal dimension for faster inference. We solve the flickering issue by replacing the LSTM layer with a 1D convolutional layer.

We investigate two distinct types of discriminators in this work. The image discriminator is designed to evaluate the authenticity of a single input image, while the video discriminator is trained to classify a sequence of frames concatenated along the channel dimension as either real or fake.

As shown in Table 3, the lip sync confidence score is high when we use the image discriminator. We believe that this is because the image discriminator is designed to analyse the details of a single image, which means that the generator must focus on spatial information to deceive the discriminator. On the other hand, the video discriminator examines the authenticity of multiple frames at the same time, which requires the generator to focus on both spatial and temporal information. Based on our analysis, we conclude that the image discriminator is more suitable for our intended purpose of accurately generating lip shape, which is a spatially small region.

#### 4.4.3. Orthogonality Constraint Effectiveness.

We provide further insight into the efficacy of the orthogonality constraint by visualising samples in the canonical space.

As depicted in Fig. 6, the canonical space of the model trained without orthogonality constraint contains diverse head poses, indicating the potential lack of disentanglement between identity and motion information. Additionally, when cosine similarity loss is used as the orthogonality constraint, the model produces even blurry images. On the contrary, the canonical space of FC-TFG trained with  $L_{ortho}$  in Eqn. (3) contains more unified facial motions, indicating a successful disentanglement of identity and motion information in the latent space. The quantitative results according to the different orthogonality constraints are reported in Table 4. These results strongly suggest that the orthogonality constraint plays a crucial role in achieving high-quality outcomes.

## 5. CONCLUSION AND DISCUSSION

### 5.1. Conclusion.

In this work, we propose a framework named Fully-Controllable Talking Face Generation (FC-TFG), which can generate every facial expression while synchronising lip movements with the input audio sources. Our framework is carefully designed to disentangle the latent space of StyleGAN into the canonical space and the multimodal motion space. This disentanglement enables the generation of more detailed and controllable facial animations while avoiding the unwanted mixing of different types of conditions. With various experiments, we prove that the proposed method is highly effective, achieving state-of-the-art results in both qualitative and quantitative evaluations of generated video quality. The potential of FC-TFG for a wide range of applications that demand precise control over various facial features is significant, such as entertainment, virtual reality, and augmented reality. It could also be useful for creating personalised digital avatars or virtual assistants that can communicate and interact with users in a more natural and realistic manner.

### 5.2. Ethical Statements.

The talking face generation model has also raised concerns about the potential misuse of deepfakes and manipulated media. The misuse could have severe consequences, including spreading false information and causing harm to individuals and communities.

To address these concerns, we will limit the usage of our model and provide access only to trusted communities such as those working on technologies beneficial to society such. Additionally, steps must be taken to ensure that the technology is used ethically and responsibly. This includes educating users on the potential risks and providing clear guidelines.

## 6. REFERENCES

- [1] Joon Son Chung, Amir Jamaludin, and Andrew Zisserman, “You said that?,” in *Proc. BMVC.*, 2017.
- [2] Hao Zhu, Huaibo Huang, Yi Li, Aihua Zheng, and Ran He, “Arbitrary talking face generation via attentional audio-visual coherence learning,” in *Proc. IJCAI*, 2020.
- [3] Lele Chen, Zhiheng Li, Ross K Maddox, Zhiyao Duan, and Chenliang Xu, “Lip movements generation at a glance,” in *Proc. ECCV*, 2018, pp. 520–535.
- [4] Hang Zhou, Yu Liu, Ziwei Liu, Ping Luo, and Xiaogang Wang, “Talking face generation by adversarially disentangled audio-visual representation,” in *Proc. AAAI*, 2019, vol. 33, pp. 9299–9306.
- [5] Konstantinos Vougioukas, Stavros Petridis, and Maja Pantic, “Realistic speech-driven facial animation with gans,” *Intl. Journal of computer vision*, vol. 128, pp. 1398–1413, 2020.
- [6] Yang Song, Jingwen Zhu, Dawei Li, Xiaolong Wang, and Hairong Qi, “Talking face generation by conditional recurrent adversarial network,” *arXiv preprint arXiv:1804.04786*, 2018.
- [7] KR Prajwal, Rudrabha Mukhopadhyay, Vinay P Nambodiri, and CV Jawahar, “A lip sync expert is all you need for speech to lip generation in the wild,” in *Proc. ACM MM*, 2020, pp. 484–492.
- [8] Se Jin Park, Minsu Kim, Joanna Hong, Jeongsoo Choi, and Yong Man Ro, “Synctalkface: Talking face generation with precise lip-syncing via audio-lip memory,” in *Proc. AAAI*, 2022, vol. 36, pp. 2062–2070.
- [9] Supasorn Suwajanakorn, Steven M Seitz, and Ira Kemelmacher-Shlizerman, “Synthesizing obama: learning lip sync from audio,” *ACM Transactions on Graphics*, vol. 36, no. 4, pp. 1–13, 2017.
- [10] Dipanjan Das, Sandika Biswas, Sanjana Sinha, and Brojeshwar Bhowmick, “Speech-driven facial animation using cascaded gans for learning of motion and texture,” in *Proc. ECCV*. Springer, 2020, pp. 408–424.
- [11] Lele Chen, Ross K Maddox, Zhiyao Duan, and Chenliang Xu, “Hierarchical cross-modal talking face generation with dynamic pixel-wise loss,” in *Proc. CVPR*, 2019, pp. 7832–7841.
- [12] Robert Anderson, Björn Stenger, Vincent Wan, and Roberto Cipolla, “An expressive text-driven 3d talking head,” in *Proc. ACM SIGGRAPH*, pp. 1–1. 2013.
- [13] Justus Thies, Mohamed Elgharib, Ayush Tewari, Christian Theobalt, and Matthias Nießner, “Neural voice puppetry: Audio-driven facial reenactment,” in *Proc. ECCV*. Springer, 2020, pp. 716–731.
- [14] Linsen Song, Wayne Wu, Chen Qian, Ran He, and Chen Change Loy, “Everybody’s talkin’: Let me talk as you want,” *IEEE Transactions on Information Forensics and Security*, vol. 17, pp. 585–598, 2022.
- [15] Lele Chen, Guofeng Cui, Celong Liu, Zhong Li, Ziyi Kou, Yi Xu, and Chenliang Xu, “Talking-head generation with rhythmic head motion,” in *Proc. ECCV*. Springer, 2020, pp. 35–51.
- [16] Yang Zhou, Xintong Han, Eli Shechtman, Jose Echevarria, Evangelos Kalogerakis, and Dingzeyu Li, “Makeltalk: speaker-aware talking-head animation,” *ACM Transactions On Graphics*, vol. 39, no. 6, pp. 1–15, 2020.
- [17] Alexander Richard, Colin Lea, Shugao Ma, Jurgen Gall, Fernando De la Torre, and Yaser Sheikh, “Audio-and gaze-driven facial animation of codec avatars,” in *Proc. WACV*, 2021, pp. 41–50.
- [18] Xinya Ji, Hang Zhou, Kaisiyuan Wang, Wayne Wu, Chen Change Loy, Xun Cao, and Feng Xu, “Audio-driven emotional video portraits,” in *Proc. CVPR*, 2021, pp. 14080–14089.
- [19] Suzhen Wang, Lincheng Li, Yu Ding, and Xin Yu, “One-shot talking face generation from single-speaker audio-visual correlation learning,” in *Proc. AAAI*, 2022, vol. 36, pp. 2531–2539.
- [20] Hang Zhou, Yasheng Sun, Wayne Wu, Chen Change Loy, Xiaogang Wang, and Ziwei Liu, “Pose-controllable talking face generation by implicitly modularized audio-visual representation,” in *Proc. CVPR*, 2021, pp. 4176–4186.
- [21] Borong Liang, Yan Pan, Zhizhi Guo, Hang Zhou, Zhibin Hong, Xiaoguang Han, Junyu Han, Jingtuo Liu, Errui Ding, and Jingdong Wang, “Expressive talking head generation with granular audio-visual control,” in *Proc. CVPR*, 2022, pp. 3387–3396.
- [22] Dongchan Min, Minyoung Song, and Sung Ju Hwang, “Styletalker: One-shot style-based audio-driven talking head video generation,” *arXiv preprint arXiv:2208.10922*, 2022.
- [23] Lele Chen, Guofeng Cui, Ziyi Kou, Haitian Zheng, and Chenliang Xu, “What comprises a good talking-head video generation?: A survey and benchmark,” *arXiv preprint arXiv:2005.03201*, 2020.

- [24] Hao Zhu, Man-Di Luo, Rui Wang, Ai-Hua Zheng, and Ran He, “Deep audio-visual learning: A survey,” *International Journal of Automation and Computing*, vol. 18, pp. 351–376, 2021.
- [25] Bo Fan, Lijuan Wang, Frank K Soong, and Lei Xie, “Photo-real talking head with deep bidirectional lstm,” in *Proc. ICASSP. IEEE*, 2015, pp. 4884–4888.
- [26] Bo Fan, Lei Xie, Shan Yang, Lijuan Wang, and Frank K Soong, “A deep bidirectional lstm approach for video-realistic talking head,” *Multimedia Tools and Applications*, vol. 75, pp. 5287–5309, 2016.
- [27] Prajwal KR, Rudrabha Mukhopadhyay, Jerin Philip, Abhishek Jha, Vinay Namboodiri, and CV Jawahar, “Towards automatic face-to-face translation,” in *Proc. ACM MM*, 2019, pp. 1428–1436.
- [28] Ran Yi, Zipeng Ye, Juyong Zhang, Hujun Bao, and Yong-Jin Liu, “Audio-driven talking face video generation with learning-based personalized head pose,” *arXiv preprint arXiv:2002.10137*, 2020.
- [29] Yu Deng, Jiaolong Yang, Sicheng Xu, Dong Chen, Yunde Jia, and Xin Tong, “Accurate 3d face reconstruction with weakly-supervised learning: From single image to image set,” in *Proc. CVPR*, 2019, pp. 0–0.
- [30] Zi-Hang Jiang, Qianyi Wu, Keyu Chen, and Juyong Zhang, “Disentangled representation learning for 3d face shape,” in *Proc. CVPR*, 2019, pp. 11957–11966.
- [31] Adrian Bulat and Georgios Tzimiropoulos, “How far are we from solving the 2d & 3d face alignment problem? (and a dataset of 230,000 3d facial landmarks),” in *Proc. ICCV*, 2017, pp. 1021–1030.
- [32] Yifeng Ma, Suzhen Wang, Zhipeng Hu, Changjie Fan, Tangjie Lv, Yu Ding, Zhidong Deng, and Xin Yu, “Styletalk: One-shot talking head generation with controllable speaking styles,” *arXiv preprint arXiv:2301.01081*, 2023.
- [33] Egor Burkov, Igor Pasechnik, Artur Grigorev, and Victor Lempitsky, “Neural head reenactment with latent pose descriptors,” in *Proc. CVPR*, 2020, pp. 13786–13795.
- [34] Yujun Shen, Jinjin Gu, Xiaoou Tang, and Bolei Zhou, “Interpreting the latent space of gans for semantic face editing,” in *Proc. CVPR*, 2020, pp. 9243–9252.
- [35] Ali Jahanian, Lucy Chai, and Phillip Isola, “On the ‘steerability’ of generative adversarial networks,” *arXiv preprint arXiv:1907.07171*, 2019.
- [36] Lore Goetschalckx, Alex Andonian, Aude Oliva, and Phillip Isola, “Ganalyze: Toward visual definitions of cognitive image properties,” in *Proc. ICCV*, 2019, pp. 5744–5753.
- [37] Andrey Voynov and Artem Babenko, “Unsupervised discovery of interpretable directions in the gan latent space,” in *Proc. ICML. PMLR*, 2020, pp. 9786–9796.
- [38] William Peebles, John Peebles, Jun-Yan Zhu, Alexei Efros, and Antonio Torralba, “The hessian penalty: A weak prior for unsupervised disentanglement,” in *Proc. ECCV. Springer*, 2020, pp. 581–597.
- [39] Yujun Shen and Bolei Zhou, “Closed-form factorization of latent semantics in gans,” in *Proc. CVPR*, 2021, pp. 1532–1540.
- [40] Guoxing Yang, Nanyi Fei, Mingyu Ding, Guangzhen Liu, Zhiwu Lu, and Tao Xiang, “L2m-gan: Learning to manipulate latent space semantics for facial attribute editing,” in *Proc. CVPR*, 2021, pp. 2951–2960.
- [41] Suzhen Wang, Lincheng Li, Yu Ding, Changjie Fan, and Xin Yu, “Audio2head: Audio-driven one-shot talking-head generation with natural head motion,” in *Proc. IJ-CAI*, 2021.
- [42] Joon Son Chung and Andrew Zisserman, “Out of time: automated lip sync in the wild,” in *Proc. ACCV. Springer*, 2017, pp. 251–263.
- [43] Elad Richardson, Yuval Alaluf, Or Patashnik, Yotam Nitzan, Yaniv Azar, Stav Shapiro, and Daniel Cohen-Or, “Encoding in style: a stylegan encoder for image-to-image translation,” in *Proc. CVPR*, 2021, pp. 2287–2296.
- [44] Jiankang Deng, Jia Guo, Niannan Xue, and Stefanos Zafeiriou, “Arcface: Additive angular margin loss for deep face recognition,” in *Proc. CVPR*, 2019, pp. 4690–4699.
- [45] Richard Zhang, Phillip Isola, Alexei A Efros, Eli Shechtman, and Oliver Wang, “The unreasonable effectiveness of deep features as a perceptual metric,” in *Proc. CVPR*, 2018, pp. 586–595.
- [46] Karen Simonyan and Andrew Zisserman, “Very deep convolutional networks for large-scale image recognition,” in *Proc. ICLR*, 2015.
- [47] Tero Karras, Samuli Laine, Miika Aittala, Janne Hellsten, Jaakko Lehtinen, and Timo Aila, “Analyzing and improving the image quality of stylegan,” in *Proc. CVPR*, 2020, pp. 8110–8119.
- [48] Ian Goodfellow, Jean Pouget-Abadie, Mehdi Mirza, Bing Xu, David Warde-Farley, Sherjil Ozair, Aaron Courville, and Yoshua Bengio, “Generative adversarial networks,” *Communications of the ACM*, vol. 63, no. 11, pp. 139–144, 2020.

- [49] Joon Son Chung, Arsha Nagrani, and Andrew Zisserman, “Voxceleb2: Deep speaker recognition,” in *Proc. Interspeech*, 2018.
- [50] Kaisiyuan Wang, Qianyi Wu, Linsen Song, Zhuoqian Yang, Wayne Wu, Chen Qian, Ran He, Yu Qiao, and Chen Change Loy, “Mead: A large-scale audio-visual dataset for emotional talking-face generation,” in *Proc. ECCV*. Springer, 2020, pp. 700–717.
- [51] Aliaksandr Siarohin, Stéphane Lathuilière, Sergey Tulyakov, Elisa Ricci, and Nicu Sebe, “First order motion model for image animation,” in *NeurIPS*, 2019, vol. 32.
- [52] Yuval Alaluf, Omer Tov, Ron Mokady, Rinon Gal, and Amit Bermano, “Hyperstyle: Stylegan inversion with hypernetworks for real image editing,” in *Proc. CVPR*, 2022, pp. 18511–18521.
- [53] Omer Tov, Yuval Alaluf, Yotam Nitzan, Or Patashnik, and Daniel Cohen-Or, “Designing an encoder for stylegan image manipulation,” *ACM Transactions on Graphics*, vol. 40, no. 4, pp. 1–14, 2021.
- [54] Diederik P Kingma and Jimmy Ba, “Adam: A method for stochastic optimization,” *arXiv preprint arXiv:1412.6980*, 2014.
- [55] Adam Paszke, Sam Gross, Francisco Massa, Adam Lerer, James Bradbury, Gregory Chanan, Trevor Killeen, Zeming Lin, Natalia Gimelshein, Luca Antiga, et al., “Pytorch: An imperative style, high-performance deep learning library,” 2019.
- [56] Zhou Wang, Alan C Bovik, Hamid R Sheikh, and Eero P Simoncelli, “Image quality assessment: from error visibility to structural similarity,” *IEEE transactions on image processing*, vol. 13, no. 4, pp. 600–612, 2004.
- [57] Zhou Wang, Eero P Simoncelli, and Alan C Bovik, “Multiscale structural similarity for image quality assessment,” in *The Asilomar Conference on Signals, Systems & Computers*. Ieee, 2003, vol. 2, pp. 1398–1402.